

Growth and characterization of ZnO nanostructured thin films by successive ionic layer adsorption and reaction

E. EL hamri^{1*}, A. Elfanaoui¹, A. Ihlal¹, K. Bouabid¹, L. Boulkadat¹, M. Meddah¹, A. Outzourhit²

¹ *Laboratoire Matériaux et Energies Renouvelables (LMER), Université Ibn Zohr Dép. Physique, Faculté des sciences B.P.8106, Hay Dakhla, 80000 Agadir, Morocco.*

² *Laboratoire de physique des solides et des couches minces, Département de physique, Faculté des sciences Semlalia, BP:S/3293, Marrakech, Morocco*

*Corresponding author: e.elhamri@yahoo.fr

Abstract: The zinc oxide (ZnO) thin films were deposited onto the glass substrates by a novel chemical method, which is based on the alternate dipping of substrate in an alkaline zinc with ammonia formed zinc ammonia complex ($[\text{Zn}(\text{NH}_3)_4]^{2+}$) solution and double-distilled water containing H_2O_2 (1%) at room temperature. The time duration for which the substrate is dipped in the precursor solution, plays an important role and it has been shown in this work that the time period for which a substrate is dipped in dilute H_2O_2 solution, which we referred as reaction period, affects significantly on the structural, surface morphological and optical properties. The as-deposited films were annealed at 300 and 400°C for 1h in air to improve the quality of the films. The as prepared nanostructured seed layer was characterized by X-ray diffraction (XRD) and scanning electron microscopy (SEM) studies showed that the films are covered well with glass substrates and have good polycrystalline structure and crystalline levels. The film thickness effect on band gap values was investigated and band gap values were found to be within the range of 3.8 – 3.2 eV.

Keywords: zinc oxide ZnO, Thin films, SILAR, Nanostructure, Annealing and Optical properties.

I. Introduction

The semiconductor zinc oxide is recognized as one of the most important semiconductor materials which exhibits numerous characteristics that may enable its efficient utilization for various technological applications such as antireflection coatings, transparent electrodes in solar cells [1,2], gas sensors [3,4], varistors [5], electro- and photoluminescent devices [6], surface acoustic wave devices [7], piezoelectric devices [8], and others.

ZnO film is one of the most important functional oxides with direct wide band gap (3.37 eV) and large excitation binding energy (60 meV), exhibiting many interesting electrical and optical properties [9–11]. Especially, the recent discovery of ultraviolet luminescence at room temperature for ZnO microcrystallite thin films and nanorod array film [12,13], together with the intensive researches on p-type ZnO films [14,15], has stimulated immense researching interests for its promising applications in various photoelectric devices.

Many physical and chemical techniques are suitable for preparing ZnO films with nanostructures, such as molecular beam epitaxy [16], metal organic chemical vapor deposition [17], sputtering [18], electrochemical deposition (ED) [19], sol-gel [20], chemical bath deposition (CBD) [21], and successive ionic layer adsorption and reaction (SILAR) [22] etc. In view of the low production cost, less or no pollution to the

environment, and more convenient control over the deposition process, the synthesis of ZnO nanocluster films via the solution route is stressed. Among several commonly adopted solution routes for the deposition of semiconductor films such as sol-gel, CBD and SILAR, SILAR is distinguished for its layer-by-layer growing feature and separate anionic and cationic sources, which make the control over the film growth process more convenient. However, the very low deposition rate and great difficulties involved in the deposition of oxide film in SILAR have limited its commercial application [23].

In this technique a glass substrate is dipped alternately into beakers containing aqueous solutions or distilled water for the reaction to take place at the substrate surface. The substrate can be introduced into various reactants for a specific length of time depending on the nature and kinetics of the reaction. The immersion-reaction cycle can be repeated for any number of times, limited only by the inherent problems associated with the deposition technique and the substrate-thin film interface. In this paper, we report the same technique of ZnO film fabrication from ammonium zincate solution. Although Ristov et al. [24] mentioned that best quality films are obtained from ammonium zincate bath (among the four zinc complex used), details of the film growth rate on different deposition parameters were not discussed in

their work. The different deposition parameters governing the film growth process are discussed here. The structural and optic properties of the deposited films are also studied.

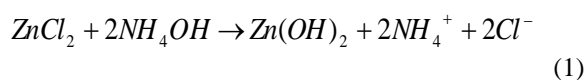
II. Experimental details

2.1. Deposition of ZnO seed layer films

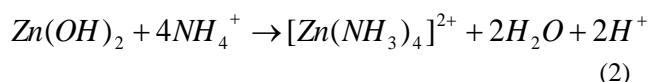
Aqueous zinc ions solution complexed with $\text{NH}_3\text{-H}_2\text{O}$ was chosen as the cation precursor, in which analytical reagents of $(\text{ZnCl}_2, 7\text{H}_2\text{O})$ and concentrated ammonia (25~28%) were used. The concentration of zinc solution is 0.01 mol/l and the molar ratio of Zn: NH_3 is 1:10 based on our optimal results. The second precursor was diluted in H_2O_2 (1%) solution which was obtained by dissolving 1 ml of H_2O_2 in 100 ml in double distilled water. In our experiment; normal microscope glass slides were chosen as substrate. Prior to use, the substrates were immersed cleaned in dilute sulfuric acid (1:10 v/v) for 10 min, and digressed in ethanol and acetone before and then rinsed with water subsequently. In short, a full deposition cycle comprises four processes, the adsorption of zinc–ammonia complex on the substrate, the formation of $\text{Zn}(\text{OH})_2$ in a standstill water, the ultrasonic rinsing of substrate to remove counter-ions and loosely bonded $\text{Zn}(\text{OH})_2$, and the immersion of substrate in hot water (90°C) to convert $\text{Zn}(\text{OH})_2$ to ZnO. The time for each process was 15, 20, 30 and 20s, respectively. In special, the withdrawing process of substrate from the hot water was carried out in about 3–5 s, to permit the rapid evaporation of water on substrate.

2.2. ZnO experimental growth

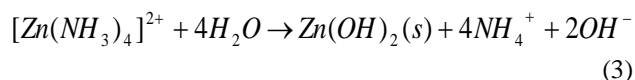
The ammonium zincate bath, used for deposition of ZnO was prepared by adding ammonium hydroxide (25% ammonia solution) to an aqueous solution of zinc chlorid ($\text{ZnCl}_2, 7\text{H}_2\text{O}$). At first, a white precipitate of zinc hydroxide $[\text{Zn}(\text{OH})_2]$ appears according to the reaction:



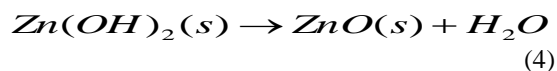
However, on further addition of ammonia, the precipitate dissolved forming the $(\text{NH}_4)_2\text{ZnO}_2$ bath following the reaction:



When the glass substrate is immersed in the solution above, these zinc complex ions get adsorbed on the substrate thanks to the attractive forces between ions in the solution and the surface of the substrate. These forces may be Van der Waals, cohesive or chemical attraction [25]. Then, the glass substrate is immersed in hot water, and the $[\text{Zn}(\text{NH}_3)_4]^{2+}$ complex decomposes, forming $\text{Zn}(\text{OH})_2$:



The reaction occurring on the surface of the substrate leading to the formation of ZnO from ammonium zincate bath is:



The substrates were dried and stored in desiccators. For investigation of the annealing effect, the films were annealed at temperature of 300 and 400°C in air during 1 h. The crystalline structure was characterized by an X-ray diffractometer (Siemens D5000 XRD unit) in 2θ range from 25° to 70° by 0.02°s^{-1} steps operating at 40 kV accelerating voltage and 40 mA current using Cu Ka radiation source. The incident angle was kept constant at 0.5° throughout the experimentation. In order to study the optical transmission properties of the generated films, the transmission spectra were measured by Lambda 45 UV/VIS/NIR PerkinElmer spectrophotometer.

3. Results and discussion

3.1. X-ray diffraction analysis

Fig.1: shows the evolution of XRD pattern of SILAR grown ZnO nanostructured seed layer deposited on glass substrate and annealed at different temperature in ambient air. The XRD pattern from all the deposition cycles has shown a major diffraction peaks at 2θ equal to $34,64^\circ$, which is corresponding to (002) orientation of hexagonal wurtzite structure (JCPDS 36-1451) and good crystallinity.

We observed that all of the films have the same crystal structure but the intensities and full width at half maximum (FWHM) values of these peaks changed with different annealing temperature and numbers of deposit. The diffraction peak intensities increased with an increasing annealing temperature (see Fig.1) and number of deposition cycles (see Fig.2). These changes may be attributed to the improvement of crystallinity of the films by annealing temperature and film thickness.

It is seen from Fig.2 the films growth on 30 cycle deposited seed layered substrates showed higher intensity along the (0 0 2) directions indicating that this particular seed layer condition is more suitable for the nanostructured films growth. In addition to the (0 0 2) peak, we also observed other peaks such as (100), (002), (101), (102), (103), (201), and (004) which are corresponding to the hexagonal ZnO phase. All of these results are in agreement with relevant literature [24, 25, 26].

The presence of the phase hydroxide of zinc [27] was not identified, probably because of its presence in small quantities and/or with its accumulation along the grain boundaries, or with its presence with the amorphous state [26].

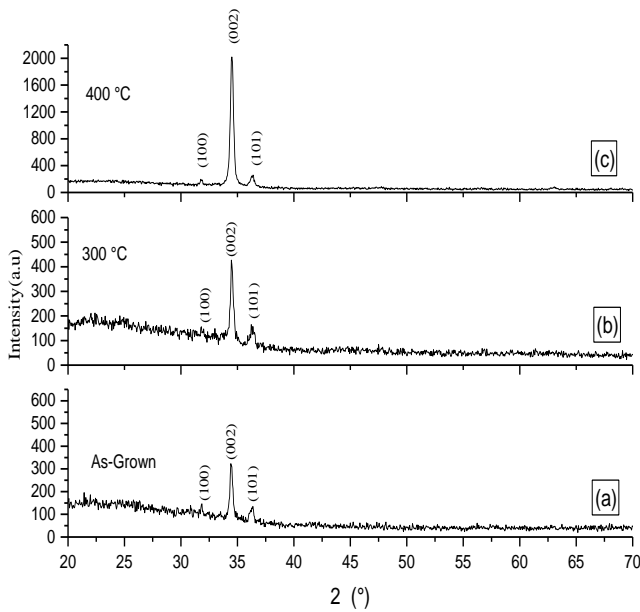


Fig.1. XRD spectra of ZnO nanostructure growth on seed layer substrate deposited at 30 cycles and annealed at different temperature.

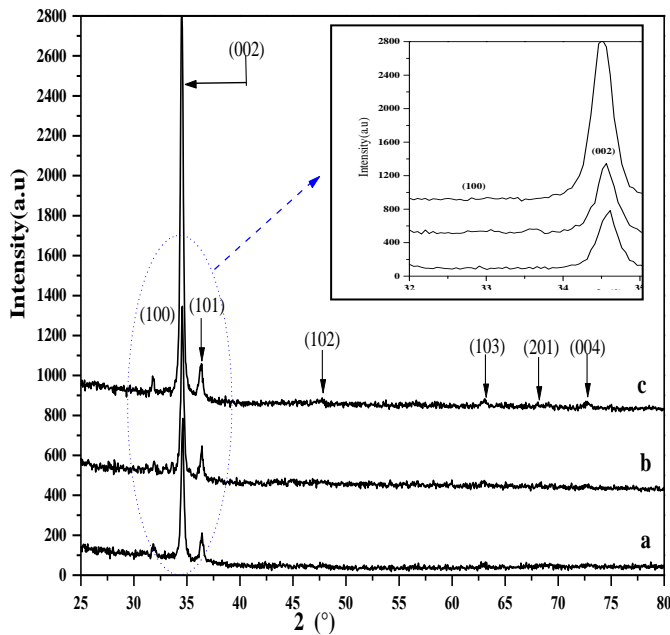


Fig. 2. XRD spectra of ZnO nanostructured seed layered thin films prepared at different deposition cycles: (a) 10, (b) 20 and (c) 30 cycles at 400°C

The grain size (D) of the prepared ZnO thin films was obtained from XRD line broadening using the Scherrer equation:

$$D = \frac{0.9\lambda}{\beta \cos\theta} \quad (1)$$

Where D is the crystal dimension perpendicular to the reflecting plane, $\lambda = 1.5406\text{\AA}$ is the wavelength of $\text{CuK}\alpha$

radiation source, β the peak full width at half maximum (FWHM), θ is the angle of the peak.

The mean crystallite size of ZnO film can be estimated from Scherrer's formula (Eq. 1), for the deposited films in 10, 20 and 30 cycles at 400°C are respectively 33.1 nm, 30.26 nm and 28.6 nm. So it can be inferred that the crystallite size of ZnO film may be primarily controlled by the deposition parameters. The effects of number of cycles are significant.

3.2. Morphology

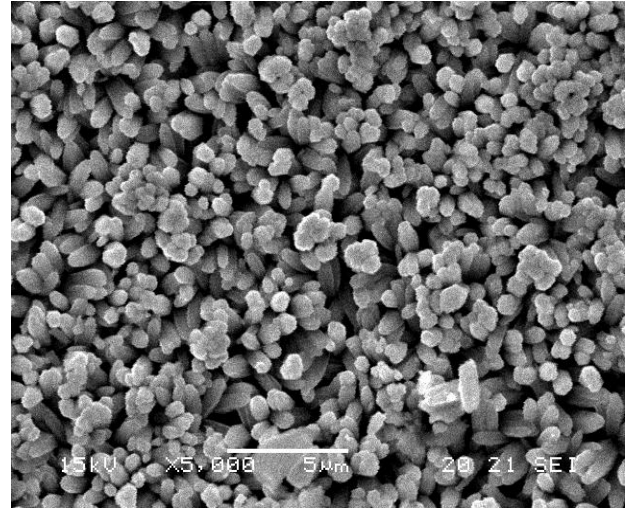


Fig.3. SEM images of ZnO thin films prepared at 30 deposition cycles and annealed at 400°C for one hour.

Fig. 3 shows SEM morphology of the surface of ZnO prepared at 30 deposition cycles and annealed at 400°C. The obtained ZnO films were smooth, transparent, continuous and homogeneous. As seen, the film is specular and formed with fine and small nano-particles with different grains sizes.

Thus from our morphology study, we concluded a fact that the distribution of dense ZnO nanostructures and the morphology is highly growth condition. We confirmed this by repeating the growth process by several times.

3.3. Optical characterization

Measurements were taken in the wavelength range 200 – 2000 nm on the deposited films. The transmission coefficient was found to be above 80% (See Fig.4) for the films obtained by 10, 20 and 30 cycles at 400°C.

The determination of the optical gap is based on the model suggested by Tauc [28] where E_g is connected to the absorption coefficient α by.

$$(\alpha h\nu)^2 = A(h\nu - E_g) \quad (2)$$

Where A is a constant, E_g is the optical gap expressed in eV and $h\nu$ is the photon energy in eV.

The plot of $(\alpha h\nu)^2$ against $(h\nu)$ shows linear part dependence. This means that ZnO films are a semiconductor type with direct transition. The band gap value E_g is determined by extrapolating the linear part of

the $(\alpha h\nu)^2$ curve towards the $(h\nu)$ axis until $(\alpha h\nu)^2 = 0$, as shown in (Fig.5).

The variation of E_g with film thickness was not noticeable. The absorption edge for the deposited film is about 330 nm, which corresponds to the optical energy bandgap of 3.76 eV. This value is in good agreement with the gap of undoped ZnO films [25].

From the results found in the Fig.5 illustrates the energy bandgap is 3.86, 3.76 and 3.70 eV. This value is in good agreement with those published by other authors [19, 26]. However, it is still higher than the optimum range for solar energy conversion. It should be reduced by adding some metallic elements such as aluminum and silver. Such work is currently undertaken in our laboratory.

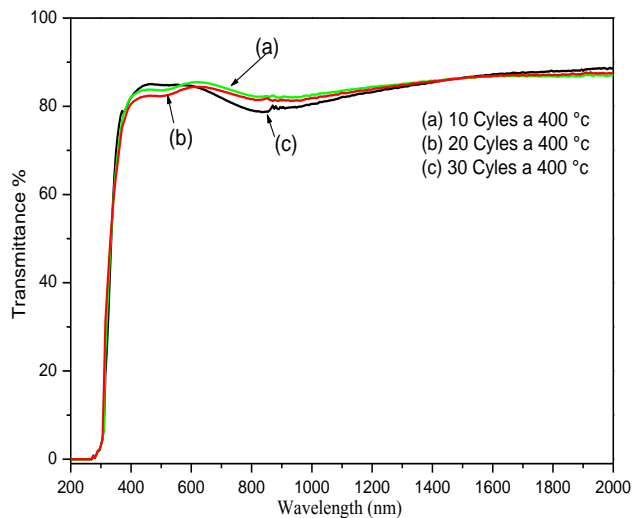


Fig.4. Transmission spectra of films obtained by 10, 20 and 30 cycles at 400°C.

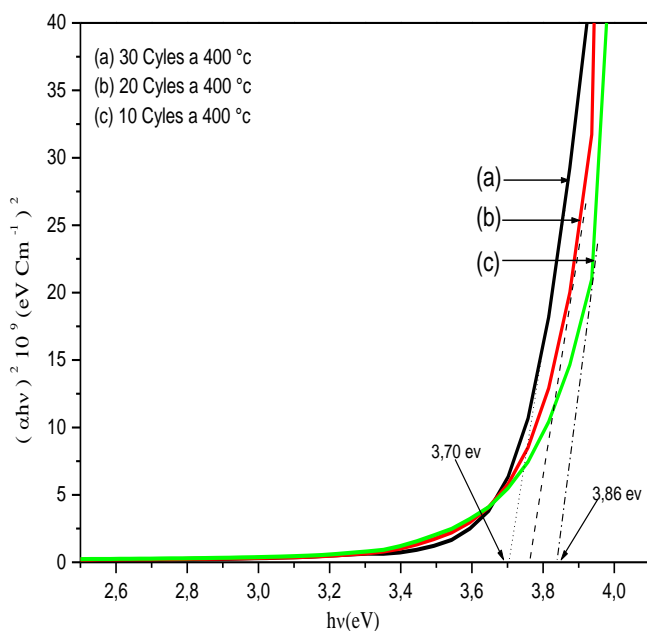


Fig.5. Graphs of $(\alpha h\nu)^2$ versus $h\nu$ for thin films prepared at different deposition cycles: (a) 10, (b) 20 and (c) 30 cycles at 400°C

This last value is in good agreement with the value 3.7 eV, which was formerly reported for highly resistive ZnO polycrystalline films [5].

IV. Conclusions

In this paper, we presented results on ZnO thin films prepared by SILAR in optimum conditions. The films obtained were milky transparent, adherent and homogeneous. The dependence of the film growth rate on the number of de cycles was studied.

We found that the number of cycles affects the grain size and the crystallinity. However, further work must be done to achieve this type of solar cells.

References

- [1] T. Ootsuka, Z. Liu, M. Osamura, Y. Fukuzawa, R. Kuroda, Y. Suzuki, N. Otogawa, T. Mise, S. Wang, Y. Hoshino, Y. Nakayama, H. Tanoue, Y. Makita, "Thin Solid Films 476 (2005) 30.
- [2] R.R. Potter, Sol. Cells 16 (1986) 521.
- [3] D.H. Yoon, G.M. Choi, Sens. Actuators, B 45 (1997) 251.
- [4] S.Y. Sheng, Z.T. Shu, Sens. Actuators, B 12 (1993) 5.
- [5] J.H. Han, D.Y. Kim, J. Europ. Ceram. Soc. 18 (1998) 765.
- [6] A. Mitra, R.K. Thareja, V. Ganesan, A. Gupta, P.K. Sahoo, V.N. Kulkarni, Appl. Surf. Sci. 174 (2001) 232.
- [7] S.H. Seo, W.C. Shin, J.S. Park, Thin Solid Films 416 (2002) 190.
- [8] S.C. Ko, Y.C. Kim, S.S. Lee, S.H. Choi, S.R. Kim, Sens. Actuators, A 103(2003) 130.
- [9] R. Konenkamp, K. Boedecker, M.C. Lux-Steiner, Appl. Phys. Lett. 77(2000) 2575.
- [10] L. Vayssieres, K. Keis, A. Hagfeldt, S.E. Lindquist, Chem. Mater. 13(2001) 4395.
- [11] M.H. Huang, Y. Wu, H. Feick, N. Tran, E. Weber, P.D. Yang, Adv.Mater. 13 (2001) 113
- [12] Z.K. Tang, G.K.L. Wong, P. Yu, M. Kawasaki, A. Ohtomo, H. Koinuma, Y. Segawa, Appl. Phys. Lett. 72 (1998) 3270.
- [13] M.H. Huang, S. Mao, H. Feick, H. Yan, Y. Wu, H. Kind, E. Weber, R. Russo, P. Yang, Science 292 (2001) 1897.
- [14] J.M. Bian, X.M. Li, X.D. Gao, W.D. Yu, L.D. Chen, Appl. Phys. Lett. 84 (2004) 541.
- [15] C.C. Lin, S.Y. Chen, S.Y. Cheng, H.Y. Lee, Appl. Phys. Lett. 84(2004) 5040.
- [16] J.K. Hang, Y. Chen, S.K. Hong, T. Yao, J. Cryst. Growth 209 (2000) 816.
- [17] J. Ye, S. Gu, S. Zhu, T. Chen, L. Hu, F. Qin, R. Zhang, Y. Shi, Y. Zheng, J. Cryst. Growth 243 (2002) 151.
- [18] E.M. Bachari, G. Baud, S.B. Amor, M. Jacquet, Thin Solid Films 348(1999) 165.
- [19] D. Gal, G. Hodes, D. Lincot, H.W. Schock, Thin Solid Films 361/362 (2000) 79.
- [20] L. Armelao, M. Fabrizio, S. Gialanella, F. Zordan, Thin Solid Films 394 (2001) 90.

- [21] T. Saeed, P. O'Brien, *Thin Solid Films* 271 (1995) 35.
- [22] Y.F. Nicolau, *Appl. Surf. Sci.* 22/23 (1985) 1061.
- [23] T.P. Niesen, M.R.D. Guire, *Solid State Ionics* 151 (2002) 61.
- [24] M. Ristov, G.J. Sinadinovski, I. Grozdanov, M. Mitreski, *Thin Solid Films* 149 (1987) 65.
- [25] M. Ali Yıldırım, Aytunç Ates_ / *Optics Communications* 283 (2010) 1370–1377
- [26] V. R. Shinde, C.D. Lokhande, R. S. Mane, Sung-Hwan, *Applied Surface Science* 245 (2005) 407.
- [27] P. Suresh Kumar , A. Dhayal Raj , D. Mangalaraj , D. Nataraj, *Applied Surface Science* 255 (2008) 2382–2387
- [28] J. Tauc, A. Menth, *J. Non-Cryst. Solids* 8–10 (1972) 569.